



Characterisation of an artesian groundwater system in the Valle de Iglesia in the Central Andes of Argentina

Ilka Hinzer¹ · Manuel Altherr¹ · Rodolfo Christiansen^{2,3} · Jürgen Schreuer¹ · Stefan Wohnlich¹

Received: 8 June 2020 / Accepted: 23 May 2021 / Published online: 4 June 2021
© The Author(s) 2021

Abstract

Despite its location in the “Arid Diagonal” of South America, the Valle de Iglesia contains a number of artesian springs, the most important of which are the Baños Pismanta thermal springs, which release water at ~45 °C. Despite the scarcity of water resources in the Valle de Iglesia, there have been few attempts to study these springs in any detail. In this study, > 50 springs are described, each characterised by small volcano-like mud structures up to 15 m tall. Hydrogeological and hydrochemical analyses of the groundwater system in the Valle de Iglesia were performed to improve our understanding of the subsurface water flow and of the connections between the subsurface water and the associated systems of faults and springs. Site measurements were made, and the concentrations of the main ions and trace elements were also determined by laboratory analysis of water samples. The samples obtained from the spring were rich in Na–HCO₃–SO₄ and Na–SO₄–HCO₃, but the surface water samples from the Agua Negra River were rich in Ca–SO₄–HCO₃. The temperature of the springs was in the range 20–45 °C. Both the temperatures and the ionic ratios are compatible with the presence of a deep hydraulic circulation system. The oxidation of sulphide minerals nearby the magmatic rocks and volcanic edifices causes the mobilisation of arsenic, which accumulates in the groundwater due to the low annual rainfall. The concentrations of arsenic in the spring water samples were therefore higher than the current limit set by the World Health Organisation, meaning that the water is not suitable for human consumption.

Keywords Argentina · Valle de Iglesia · Hydrochemistry · Mud volcano · Groundwater · Arid regions · Ionic ratios · Hydrochemical processes

Introduction

The Valle de Iglesia is located in San Juan Province in northwestern Argentina (Fig. 1a), in the “Arid Diagonal” of South America. The Arid Diagonal also contains the Atacama Desert, which is one of the driest regions on Earth. It is located between regions to the north with humidity supplied mainly by tropical circulation and regions to the south where the precipitation is influenced by southwesterlies (Abraham de Vazquez et al. 2000). Despite its location in the Arid

Diagonal, a number of freshwater springs supply water to the Valle de Iglesia all year round, and the water from these springs is important for irrigation and human consumption. However, the sources of the water that supplies the springs have hardly been studied (C.R.A.S. 1982; Pesce and Miranda 2003), and the proper assessment of the spatial flow pattern and quality of the water is important in order to protect the health of the local population. Many of the springs are located on the flanks or summits of small conical mounds that resemble miniature stratovolcanoes. We will refer to these features as “mud volcanoes” (MVs), which Dimitrov (2002) found to have been created by clay material ejected onto the Earth’s surface or the ocean floor. The clay material is transported as sludge to the surface due to high pressure and escaping gases, and the sludge is deposited around the outlet to create a layered conical structure. Kopf (2002) compiled a detailed catalogue of MVs around the world. Tinivella and Giustiniani (2012) described MVs in different geological environments, including compression zones,

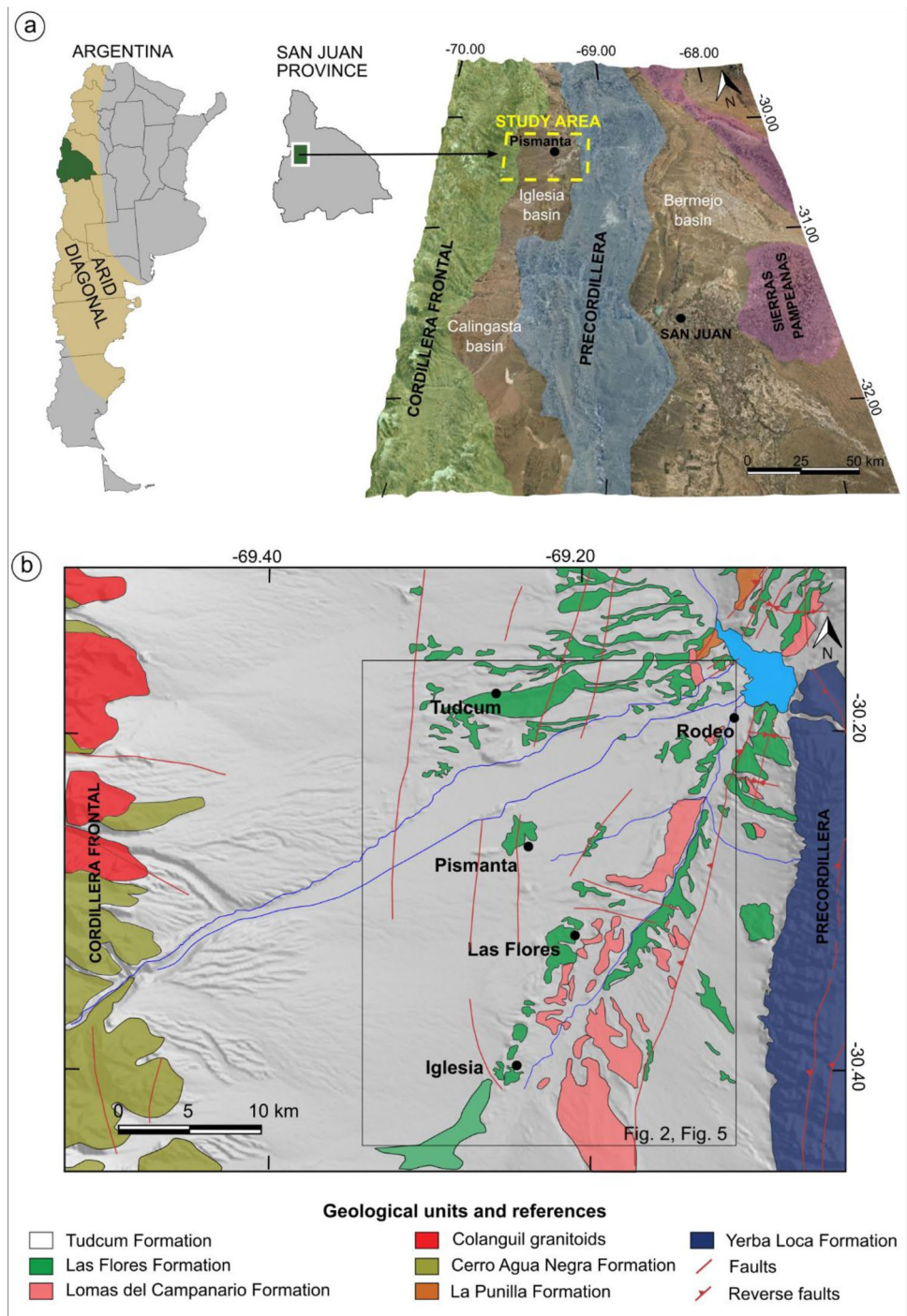
✉ Ilka Hinzer
ilka.hinzer@rub.de

¹ Institute of Geology, Mineralogy and Geophysics, Ruhr Universität Bochum, Bochum, Germany

² Universidad Nacional de San Juan, San Juan, Argentina

³ Consejo Nacional de Investigaciones Científicas y Técnicas (CONICET), Buenos Aires, Argentina

Fig. 1 Study area. **a** Location of the study area. **b** Geological map of the Valle de Iglesia. Morphotectonic areas: the Cordillera Frontal (west), where igneous rocks dominate, the Valle de Iglesia (center) and the Precordillera (east), where sedimentary and volcanic deposits are dominant



accretionary complexes, fold belts, sedimentary basins, and active plate boundaries. Mazzini and Etiope (2017) concluded that MVs are associated with active plate margins. At first sight, the springs in the Valle de Iglesia fit the definitions of Dimitrov (2002) and Tinivella and Giustiniani (2012), even though there is little or no escape of gas in the Valle de Iglesia (Pesce and Miranda 2003), and the sediment loads are very low compared with those described in the

definitions by Dimitrov (2002) and Tinivella and Giustiniani (2012).

The origins of the MVs in the Valle de Iglesia are still not well-understood, but it has been assumed that they were produced due to seismic events (Perucca and Bastias 2005; Perucca and Moreiras 2006). The Valle de Iglesia is in the Central Andes, which is one of the most seismically active areas in Argentina, having been affected by at least six

destructive earthquakes ($M \geq 6$) within a radius of < 250 km over the last 150 years (Gregori and Christiansen 2017). Sand volcanoes and new springs have been found in some parts of San Juan Province after strong earthquakes (Perucca and Bastias 2005; Perucca and Moreiras 2006). The aim of the present study was to characterise hydrogeologically and hydrogeochemically the groundwater system in the Valle de Iglesia to identify possible subsurface flow paths within the aquifers in the valley and the connections of the flow paths with fault systems, MVs, and springs in the area. To achieve this, the concentrations of major ions and trace elements in samples of water from the MVs and the Agua Negra River were determined using standard methods. The results were used to assess the circulation pattern and interactions along the flow paths between the groundwater and among the minerals in the rocks and soil. The problem of contamination by arsenic in northwestern Argentina is well known (Concha et al. 2010; O'Reilly et al. 2010), therefore the arsenic concentrations in the groundwater were determined to assess the suitability of the water for human consumption.

Location and geological setting

The study area in the Valle de Iglesia was roughly delimited by the villages of Tudcum and Rodeo to the north and the village of Iglesia to the south (Fig. 1b). The area has a mean altitude of 1800 m above sea level. Among several thermal springs and MVs within the study area, the best investigated MVs in this study are the ones around Baños Pismanta (e.g., C.R.A.S 1982). The valley is oriented north–south and can be considered to be an intramontane tectonic basin (Cloetingh et al. 1997) bordered by the Cordillera Frontal to the west and the Precordillera to the east (Fig. 1a). The part of the Cordillera Frontal close to the study area is dominated by the Agua Negra Formation, which consists of Paleozoic marine sedimentary rocks such as lutites, sandstones, limestones, and conglomerates (Polanski 1970). The area also contains igneous rocks such as the Permian Concota and Agua Negra granites, Permian to Triassic tuffs, agglomerates, and Choiyoi group ignimbrites (Yrigoyen 1972; Lambías and Sato 1990). The Precordillera mainly consists of marine deposits and thick Cambrian and Middle Ordovician carbonate formations (Keller et al. 1998; Keller 1999; Buggisch et al. 2003). Silicoclastic deposits (e.g., conglomerates, lutites, and sandstones) predominate, but pillow lavas, gabbros, and basalts from the late Ordovician are also present (Rolleri and Baldis 1967; Baldis and Chebli 1969; Baldis 1975).

The basin is filled with Neogene and Paleogene sedimentary rocks (Wetten 1975a, b; Contreras et al. 1990; Gagliardo et al. 2001). The sedimentary fill is thickest (3000–4000 m) in the southern part of the basin (Gonzalez et al. 2020). The

oldest basin-filling materials are known as the Iglesia Group, which contains Miocene pyroclastic rocks of the Lomas del Campanario Formation overlain by Pliocene clays, silts, and sandstones, which are interspersed in places with layers of gypsum of the Las Flores Formation (Perucca and Martos 2012). The youngest rocks are Pleistocene conglomerates and litharenites in the Iglesia (Cardó and Diaz 1999) and Tudcum Formations (Furque 1979), which are partly covered by alluvial and aeolian gravel and sand (Heredia et al. 2002).

Tectonic evolution and development of the area has been studied extensively (Beer et al. 1990; Jordan et al. 1993; Ré et al. 2003; Ruskin and Jordan 2007; Gonzalez et al. 2020). Fault systems developed as a result of continuous oblique convergence and subduction of the Nazca Plate under the western margin of the South American Plate, which started during the Mesozoic (DeMets et al. 1990; Mpodozis and Ramos 1989). The Nazca Plate is currently subducting sub-horizontally at a rate of 6.3 cm/year between 28° and 32° S at a depth of ~ 100 km (Cahill and Isacks 1992; Ramos et al. 1996, 2002). The subduction becomes increasingly oblique at 30° S, and this allows strike–slip faults to occur at the regional scale (Perucca and Martos 2012). Gonzalez et al. (2020) suggested that normal fault development and syn-tensional deposition of sediment occurred between the latest part of the Oligocene and the earliest part of the Miocene to the middle of the Miocene. Horizontal extension activity in the Valle de Iglesia diminished progressively from the middle Miocene and changed to horizontal shortening and basin inversion. Seismic imaging indicates that normal faults with varying degrees of tectonic inversion are dominant features of the overall basin, which is internally drained in general.

According to C.R.A.S. (1982), there are two types of aquifers in the study area, a free cold aquifer at the Quaternary levels around 120 m deep and a confined cold–hot aquifer at deeper Neogene levels within the basin. However, the Quaternary and Neogene deposits partly interlock and overlap in many places, causing potentially complex flow paths and the mixing of water from the two aquifers. The pore aquifers consist mainly of sandy units alternating with finer clay materials and, to a lesser extent, gravel and conglomerates (C.R.A.S. 1982; Zambrano and Torres 1996). C.R.A.S. (1982) found that system recharge occurs mainly through infiltration by mountain subsurface streams through permeable formations in the Cordillera Frontal. The sediment distribution and the location of the study area in the foothills of the Andes mean that the valley is mostly characterised by confined and partly artesian groundwater. The Neogene aquifer has a reservoir temperature of 75 °C (Pesce and Miranda 2003), meaning that, at a typical geothermal gradient of 30 °C/km, it is ~ 2500 m deep. We hypothesise that reactivation and tectonic inversion of faults in the area,

as also suggested by Gonzalez et al. (2020), favour the rise of thermal water from the confined Neogene aquifer.

Methods

Georeferenced aerial images of the study area were processed and maps were created to distinguish MVs and springs from other morphological features. Grass-covered MVs with diameters of 10–50 m were identified from satellite images and verified in the field. MVs with diameters < 10 m and MVs located close together were impossible to detect from the aerial images.

Characterisation of MVs and water sampling

The soil at each MV was identified on site by taking samples using a 1 m handheld drill. The diameter and height of each MV were recorded, together with the presence of any grass. A total of 26 water samples were collected, and the concentrations of major ions and trace elements were determined in water samples from the MV springs and two samples from the Agua Negra River, which is fed by rain and meltwater from the Cordillera Frontal. Each sample was collected into a 500 mL polypropylene beaker, which was first washed with the spring water before being filled with the same water. The water was passed through a cellulose nitrate filter (pore size 0.45 µm), and the filtrate was then used to fill three 50 mL polypropylene centrifuge tubes with standing rims. Concentrated nitric acid was added to prevent precipitation of the analytes, and the tubes were then sealed. Various physicochemical parameters (temperature, pH, and electrical conductivity) of the filtered water samples were determined on site using a WTW Multi 350i multiprobe.

Chemical analysis

The concentrations of major ions in the samples were determined by ion chromatography using a Dionex ICS-1000 ion chromatography system, with each sample diluted by a factor of between five and 10. Calibration curves were prepared after analysing a series of standards containing the analytes at concentrations of 0–1, 2, 10, and 20 mg/L. The concentrations of trace elements in the water samples were determined using an Optima 8300 inductively coupled plasma optical emissions spectroscopy instrument (PerkinElmer), with each sample diluted by a factor of between five and 10. Calibration curves were prepared after analysing a series of standards containing the analytes at concentrations of 0–1, 5, 10, and 40 mg/L. The concentration of hydrogen carbonate in each sample was calculated from the charge balance error CBE (in mmol/L) using the equation:

$$\text{CBE} = \frac{\sum \text{Cations} - \sum \text{Anions}}{\sum \text{Cations} + \sum \text{Anions}} \times 100, \quad (1)$$

where $\sum \text{Cations}$ is the sum of the concentrations of all the cations and $\sum \text{Anions}$ is the sum of the concentrations of all the anions. The CBE values, hydrogen carbonate concentrations, and water sample ‘fingerprints’ were calculated using AquaChem v.5.1 software.

Results

Characterisation of the MVs

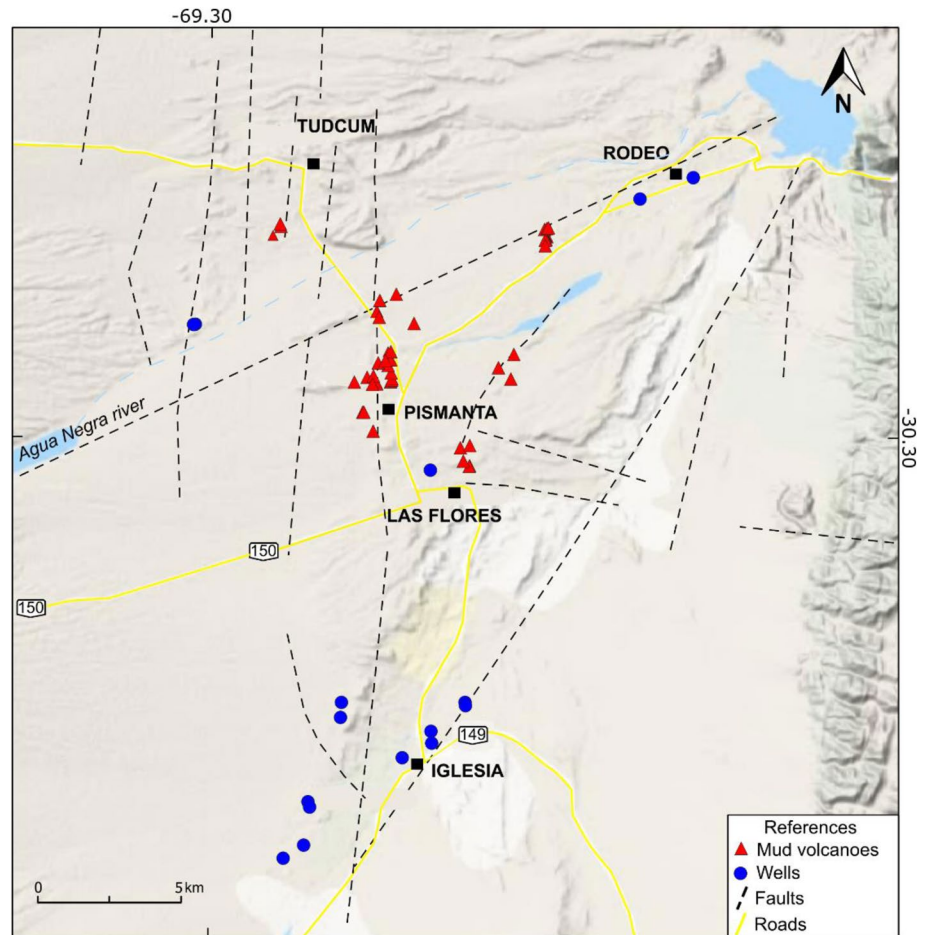
The locations of 55 MVs and 16 wells (C.R.A.S 1982) were used to analyse their possible spatial relation to the fault system of the Valle de Iglesia (Fig. 2). The MV shapes (Fig. 3) ranged from conical to flat, and some MVs were covered with vegetation. Their basal diameters were 2–50 m, with heights ranging from ~ 1 m for flat MVs to > 10 m for MVs with pronounced cones. The tops of active MVs are generally covered with reed grass, and the soil around the bases of active MVs is usually covered with a whitish–yellow saline crust. Some MVs are used to supply drinking water and water for other purposes. There are active water outlets on the tops or flanks of ~ 50% of the MVs, and the mud loads are low. Inactive MVs are often eroded to some extent.

The MVs are composed of silt and small amounts of clay and sand, and there is generally a layer of peat on top. MVs contain layers of silt interspersed with sand. A lack of water surrounding an MV-like structure indicates that evaporation is more intense than resupply, or that no water is supplied. As shown in the schematic cross-section in Fig. 3e, MVs are fed with a sludge suspension through a central feeder channel. There is a central outlet on top of the mud cone, but there may also be water outlets on the flanks that can cause the flanks to collapse.

Hydrochemical characteristics of the waters

Piper trilinear diagrams were used to determine the typology of the groundwater samples (Fig. 4). Values of the investigated parameters for all the samples are available as supplementary data. The spring water samples were in the pH range of 6.8–10.3, and the mean was pH 9.1. The electrical conductivities ranged from 442–1107 µS/cm, and the mean was 659 µS/cm. The temperatures were mostly between 14 and 27 °C but reached 43 °C around the Baños de Pismanta. The Agua Negra River surface water samples were slightly acidic to neutral (pH 6.2–7.3). The mean electrical conductivity of the Agua Negra River surface water samples was 466 µS/cm, and the temperatures were 7.5–10.5 °C.

Fig. 2 Locations of the mud volcanoes (this work) and wells (C.R.A.S. 1982) and of faults near Pismanta (Perucca and Martos 2012; Gonzalez et al. 2020)



Hydrogen carbonate, sodium, and sulphate were the dominant ions in the spring water samples. The mean HCO_3^- , Na^+ , and SO_4^{2-} concentrations were 204, 149, and 117 mg/L, respectively. In the Piper diagram (Fig. 4), the spring water sample data were on a line between hydrogen carbonate and sulphate, therefore the water samples were classed as $\text{Na-HCO}_3\text{-SO}_4$ and $\text{Na-SO}_4\text{-HCO}_3$ types. In contrast, the surface water samples were dominated by sulphate, hydrogen carbonate, and calcium. The mean SO_4^{2-} , HCO_3^- , and Ca^{2+} concentrations were 158, 153, and 83.3 mg/L, respectively. The surface water samples were therefore classed as $\text{Ca-SO}_4\text{-HCO}_3$ types. The arsenic concentrations in all the water samples from the MVs (Fig. 5) were markedly higher than the maximum allowed concentration of 10 $\mu\text{g/L}$ set by the World Health Organisation (WHO 2011). The mean arsenic concentration was $\sim 250 \mu\text{g/L}$, and the maximum was 1000 $\mu\text{g/L}$.

Ionic ratios, Gibbs plot and possible processes of spring waters and surface waters

The ionic ratio can be used to indicate the occurrence of certain processes relevant to water quality and can help identify

the source of water (Jebreen et al. 2018). The $\text{Na}:\text{Cl}$ ratio is usually used to identify halite dissolution or saline intrusion (Srinivasamoorthy et al. 2011). Some ionic ratios for the samples are shown in Fig. 6. The sodium and chloride concentrations were linearly related (Fig. 6a). Sodium and hydrogen carbonate were generally dominant, which is a characteristic of water affected by water–rock interactions. The hydrogen carbonate concentrations were higher than the sodium concentrations (Fig. 6b), suggesting that silicate weathering was one of the dominant reactions affecting the spring water. The plots of the $\text{Na}^+ + \text{K}^+$ concentrations against the SO_4^{2-} concentrations (Fig. 6c) and the $\text{Ca}^{2+} + \text{Mg}^{2+}$ concentrations against the SO_4^{2-} concentrations (Fig. 6d) indicate that Ca^{2+} was more enriched in the surface water than in the spring water, and that water–rock interactions may thus have occurred while the water was flowing. The line fitted to a plot of the $\text{Ca}^{2+} + \text{Mg}^{2+}$ concentrations against the $\text{Na}^+ + \text{K}^+$ concentrations (Fig. 6e) was almost horizontal, suggesting that Ca^{2+} and Mg^{2+} had different sources from Na^+ and K^+ . Ion exchange reactions could have occurred in the system, therefore the relationship between the $\text{Na}^+ - \text{Cl}^-$ concentration and $\text{Ca}^{2+} + \text{Mg}^{2+} - \text{SO}_4^{2-} - \text{HCO}_3^-$ concentration was assessed

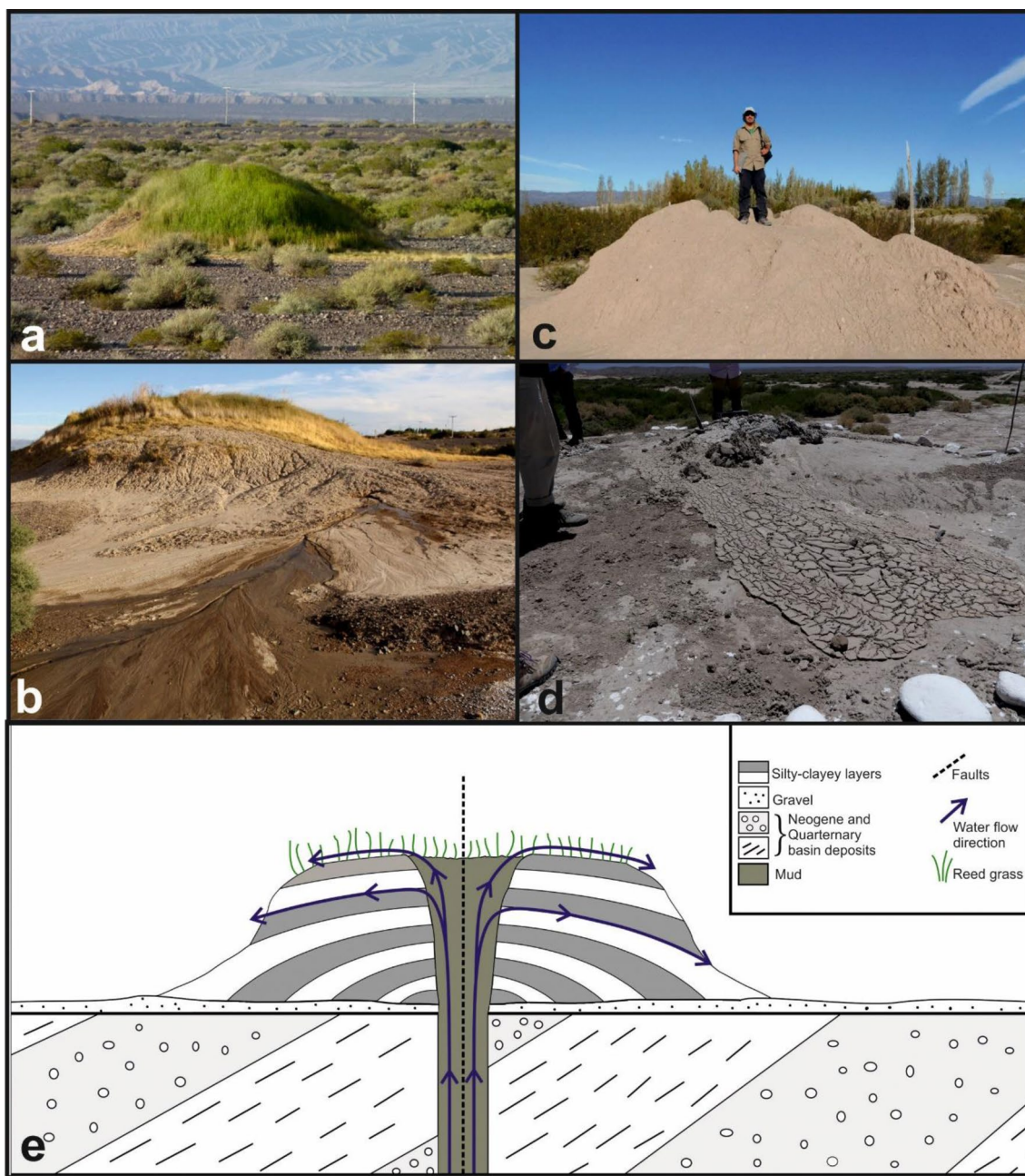


Fig. 3 Selected mud volcano types in the study area. **a** Conical mud volcano covered with grass. **b** Active mud volcano. **c** Active mud volcano with eroded flanks. **d** Mud-flow ejection from a mud volcano

after an earthquake. **e** Hypothetical cross section of a typical mud volcano in the study area (with layers eroded from the mud volcano)

(Fig. 6f). The $\text{Na}^+ - \text{Cl}^-$ concentration was defined as the concentration of Na^+ not related to halite dissolution or precipitation. The $\text{Ca}^{2+} + \text{Mg}^{2+} - \text{SO}_4^{2-} - \text{HCO}_3^-$ concentration was defined as the $\text{Ca}^{2+} + \text{Mg}^{2+}$ concentration not related to gypsum, calcite, or dolomite dissolution or precipitation. The relationship was linear, indicating that all of the major cations participated in ion exchange reactions. Gibbs

(1970) plots (Fig. 7) were also prepared in order to allow possible hydrochemical processes affecting the water (e.g., water–rock interactions, precipitation, and evaporation) to be assessed separately. The compositions of the water samples from the study area were mostly in the water–rock interaction domain, supporting the above findings on the dominant chemical processes affecting the water.

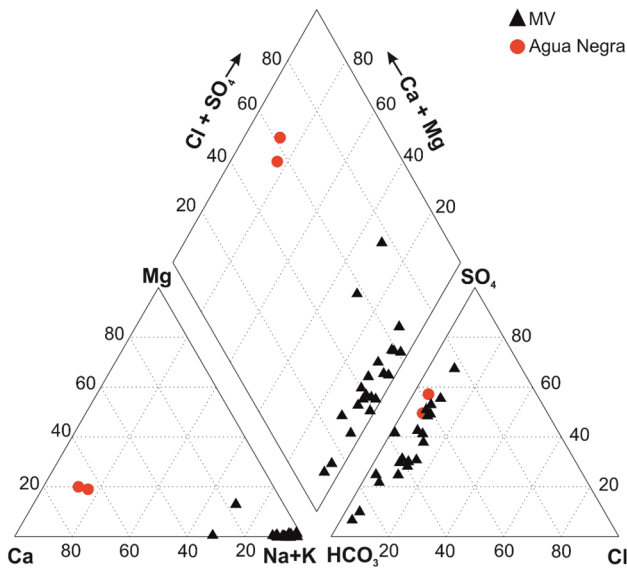


Fig. 4 Piper plot for the spring water samples from the mud volcanoes and surface water samples from the Agua Negra River

Discussion

The spatial correlation between the MVs and faults in the study area (Fig. 2) suggest a possible fault–MV relationship. Perucca and Martos (2012) found clear geomorphological evidence (offset rivers and alluvial fans, sag ponds, escarpments, and aligned springs) of Quaternary faulting for tens of kilometres in the Valle de Iglesia. Local residents have observed spring water turning cloudy for a period of time and previously inactive MVs producing flowing mud after an earthquake has been felt, indicating soil softening caused by seismic events (Fig. 3d). Therefore, increased MV activity after an earthquake in the Valle de Iglesia would be associated with a loss of rock cohesion and injection of liquefied material caused by a pressure gradient. This phenomenon has been described fully in previous publications (Kopf 2008; Manga et al. 2009; Rudolph and Manga 2012).

The internal structures of the MVs (alternating layers of silt and sand) indicate that the water flow rates or water levels in the MVs fluctuate and the amounts of sediment ejected associated with such fluctuations also fluctuate. This led us to develop the following hypotheses. During warm seasons, meltwater from the Frontal Cordillera infiltrates the

Fig. 5 Arsenic concentrations in the spring water samples from the study area [faults identified by Perucca and Martos (2012) and Gonzalez et al. (2020)]

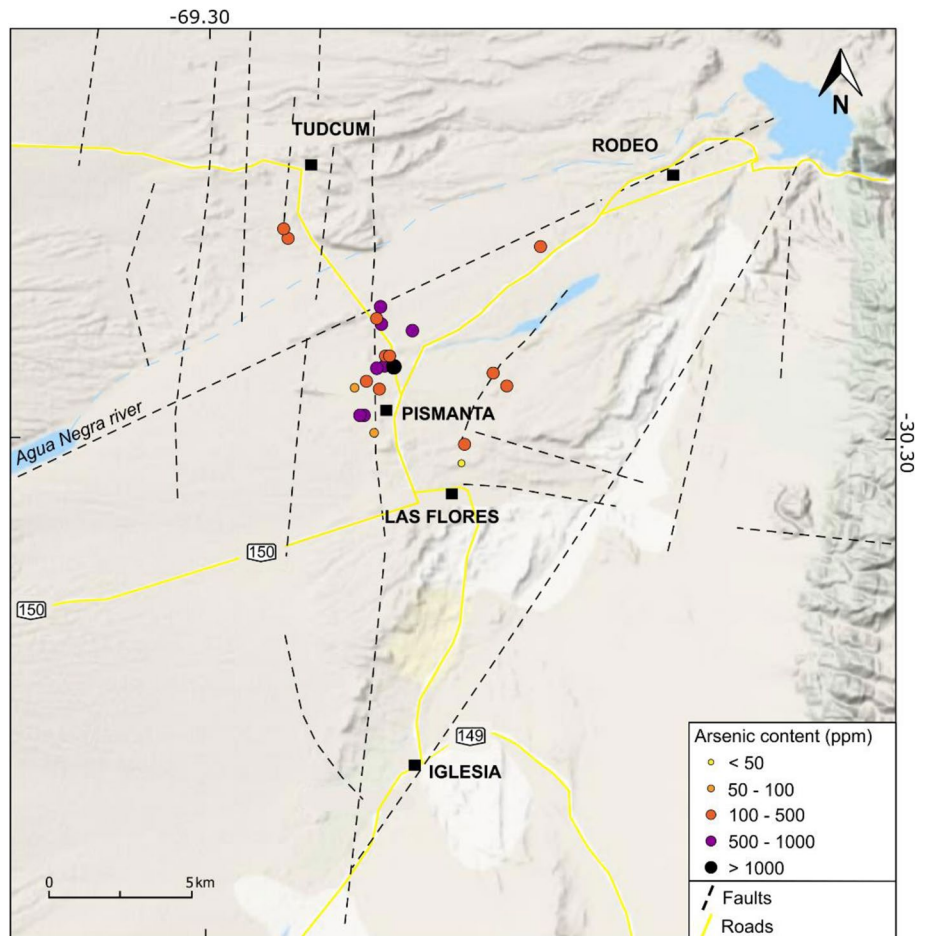
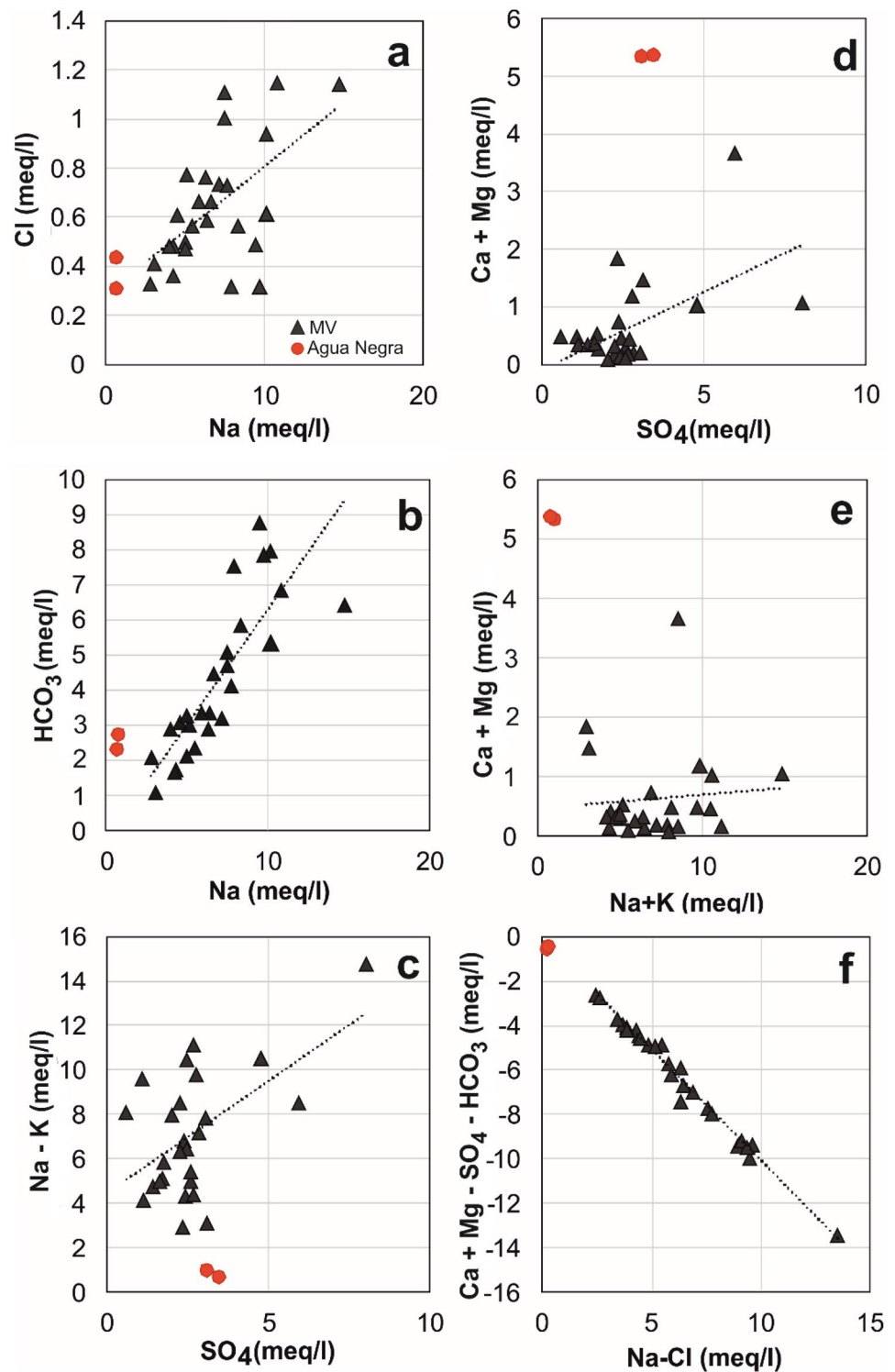


Fig. 6 Ionic ratios of spring waters (MVs) and surface waters (Agua Negra River): **a** Na^+ vs. Cl^- , **b** Na^+ vs. HCO_3^- , **c** SO_4^{2-} vs. $\text{Na}^+ + \text{K}^+$, **d** SO_4^{2-} vs. $\text{Ca}^{2+} + \text{Mg}^{2+}$, **e** $\text{Na}^+ + \text{K}^+$ vs. $\text{Ca}^{2+} + \text{Mg}^{2+}$, **f** $\text{Na}^+ - \text{Cl}^-$ vs. $\text{Ca}^{2+} - \text{Mg}^{2+} - \text{SO}_4^{2-} - \text{HCO}_3^-$



aquifer, increasing the water flow rate. During and after an earthquake, coarse sediment (e.g., sand) is released from faults and the bedrock and deposited on the surface. This episodic injection of mud and sand is reflected in the growth of grass on the MVs. A low flow rate and lack of (or low level of) mud deposition allows vegetation to grow without

being covered by sediment between strong earthquakes. Satellite images (Fig. 8) indicate that the MVs remain covered with vegetation in all seasons, pointing to a continuous supply of water. A lack of gas emissions from the MVs can be explained by the semi-arid environment and seasonal precipitation that occurred when the Valle de Iglesia strata

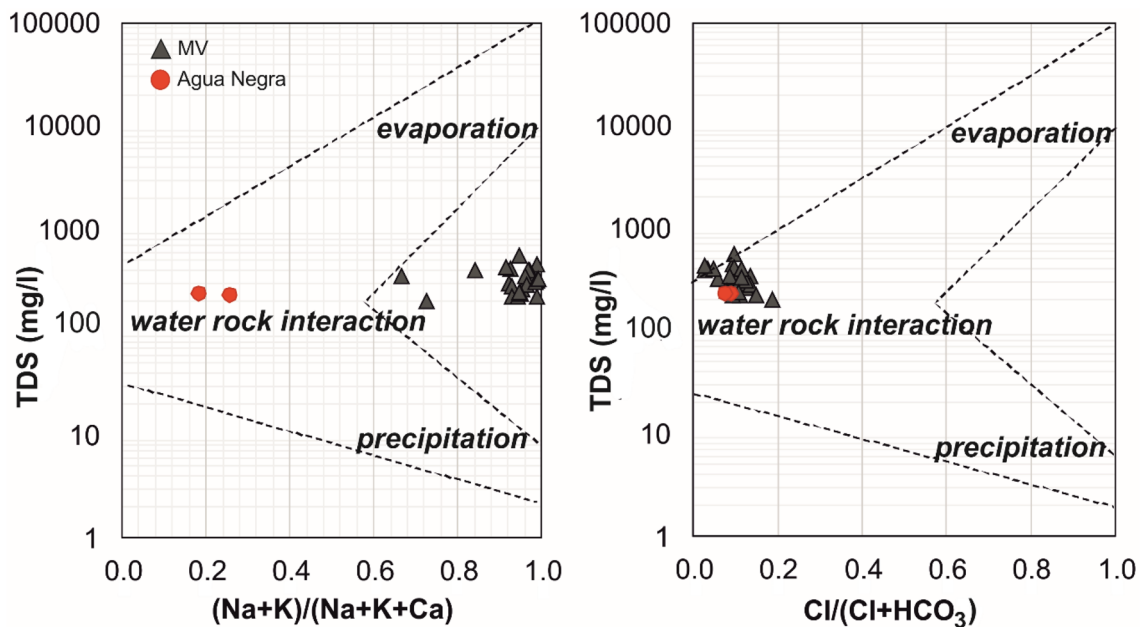


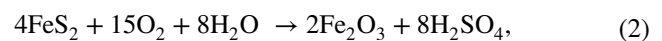
Fig. 7 Gibbs plots for the spring water samples (MV) and surface water samples (from the Agua Negra River), indicating that water–rock interactions were important processes affecting the water in the study area

accumulated (Ruskin and Jordan 2007), preventing organic matter accumulating in the area.

The chemical compositions of the water samples obtained from the MVs were very different from the chemical compositions of the water samples from the wells investigated by C.R.A.S. (1982) and from the chemical compositions of the samples from the Agua Negra River (see the supplementary table). In particular, there were marked differences between the pH and Ca^{2+} , Mg^{2+} , and SO_4^{2-} concentrations. The Ca^{2+} and Mg^{2+} concentrations were much higher in the surface water and well water samples than in the spring water samples. The low Ca^{2+} and Mg^{2+} concentrations in the spring water samples were characteristic of non-magmatic geothermal fluids. Non-thermal water usually contains Ca^{2+} at a relatively high concentration (Moeck 2014). We, therefore, conclude that non-thermal well and surface water is supplied by the Quaternary aquifer, and thermal spring water is supplied by the Neogene aquifer. Pesce and Miranda (2003) found that high water temperatures of certain springs were caused by a heat reservoir with a mean temperature of ~ 75 °C (determined using a Na–K–Ca/quartz geothermometer). The differences in the temperatures of the spring water samples are probably caused by different ascent rates and by mixing with water supplied by the Quaternary aquifer. Water released through the artificially created hot water springs in the Baños de Pismanta reaches the surface quickly through boreholes and hardly cools at all. At the other MVs, the water probably flows along faults to the surface much

more slowly and loses heat along the way. The differences in temperature may also be caused by differences in the distances between the MVs and the heat reservoir, in that outlets with higher temperatures are closer to the reservoir than those with lower temperatures. This needs to be confirmed by further investigations involving drilling or numerical modelling.

No marked differences in the chemistry of the spring water samples were found. The spring water samples were all either Na– HCO_3 – SO_4 or Na– HCO_3 – SO_4 types. The surface water and well water samples were Ca– SO_4 – HCO_3 types, suggesting that the springs are all fed by the same system or reservoir in which the ion exchange reactions occur, and that this controls the ion distribution. Silicate weathering appears to be a dominant reaction for the flow paths for both the surface water and spring water, and acids may therefore have formed through sulphide (supplied, for example, by ignimbrites in the Agua Negra mountain range) oxidation and CO_2 (in the atmosphere or soil) dissolution through the reactions shown below (Meybeck 1987; Drever 1996):



which accelerates the weathering of minerals like feldspars and calcite:

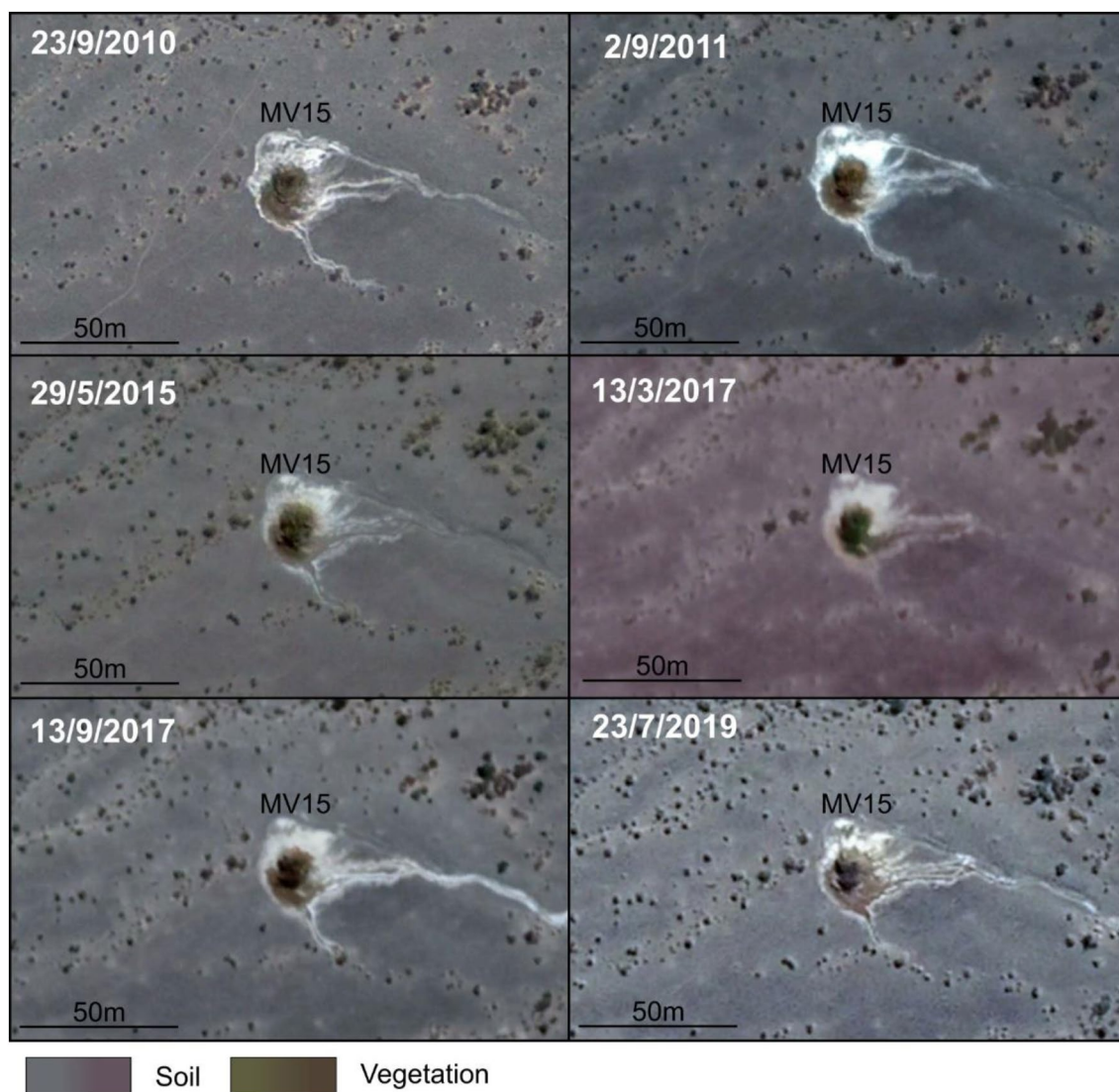
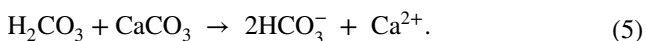
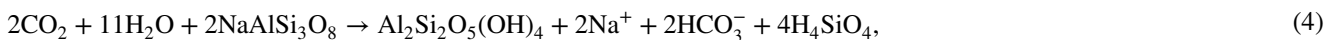


Fig. 8 Satellite images showing continuous vegetation on the top of MV15 (Image © CNES/Airbus)

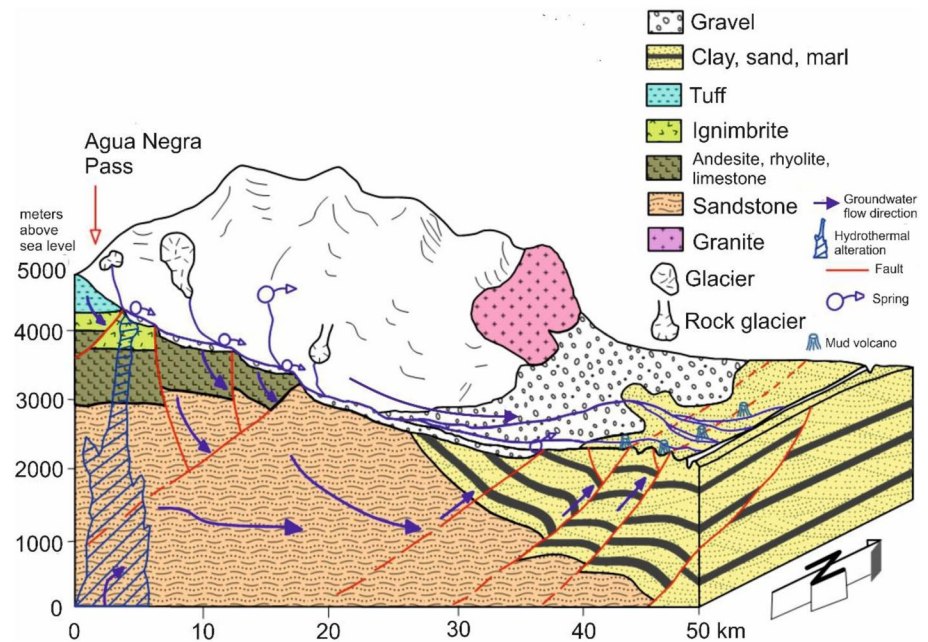


In summary, sulphide oxidation and CO_2 dissolution caused acid to form, which in turn caused mineral weathering and enriched Ca^{2+} and Na^+ in the surface water. Gonzalez et al. (2020) suggested that faults and seismic activity in the area cause interlocking and mixing of the sediments in the area. This could cause various weathering and water–rock interactions with the groundwater and sediment within the flow path. The different water temperatures in different locations also affect the reactions that occur. The solubility product is higher at higher temperatures and lower

at lower temperatures. Mixing and ion exchange reactions can take place in the subsurface. Different reactions in the flow path can cause similar ionic ratios but different total concentrations.

The results of trace element analysis indicate that the arsenic concentrations in the spring water samples were high, which matched the results of previous studies performed around San Juan (O'Reilly et al. 2010) and Salta Province in northwestern Argentina (Concha et al. 2010). All the spring water samples contained arsenic concentrations higher than the limit set by the World Health Organisation. The high arsenic concentrations in the spring water in San Juan and the Valle de Iglesia are probably geogenic.

Fig. 9 Hydrogeological model for the Valle de Iglesia basin



Volcanic activity in the study area has increased the mixing of Quaternary loess deposits with rhyolitic and dacitic ash that contains sulphide minerals and arsenic. These minerals are sensitive to oxidation. Silicate and carbonate weathering occurs under arid conditions. This may increase the pH of the water (Smedley and Kinniburgh 2002). The elevated pH makes arsenic more soluble in water and therefore causes arsenic to be leached from the sediment. However, groundwater flow is relatively low in the arid study area, meaning that arsenic accumulates in the circulation system. A schematic of the proposed hydrogeological model for the area is shown in Fig. 9.

Conclusions

A close relationship was found between MVs and thermal water in the Valle de Iglesia in the Central Andes of Argentina. Hydrochemical characterisation of water samples indicates that the properties of the thermal water released at the MVs are different from the properties of water in the rivers and wells in the study area. The study area has a complex geothermal and deep circulation system comprising a variety of water–rock interactions. There are two aquifers near Pismanta, a free cold aquifer limited to Quaternary strata and a confined hot aquifer limited to the lower Neogene strata. Water in the area is supplied by the Cordillera Frontal, from which rain and meltwater flow via side streams into the Agua Negra River. At the edge of the Cordillera Frontal, water infiltrates at least one relatively permeable aquifer in the Valle de Iglesia. The flowing water transports sediment particles from the subsurface to the surface, increasing the mud

and sand load after strong seismic events. The sediment is deposited on the surface, mostly as MVs. All the water samples were similar, indicating that there is one large coherent system in which different reactions take place. The chemical processes controlling the water are mostly ion exchange and water–rock interactions. The high arsenic concentrations in the water could be a hazard if the water is consumed by humans or put to industrial use.

Supplementary Information The online version contains supplementary material available at <https://doi.org/10.1007/s00531-021-02058-0>.

Acknowledgements The authors would like to thank PD Dr. Andre Banning for scientific support and discussion about hydrogeochemical data.

Author contributions IH collected data and samples in the field, elaborated and analysed all hydrochemical data and designed a first draft of the manuscript. MA collected data and samples in the field, located all found springs and provided and elaborated soil samples and data. RC helped to draft the manuscript, wrote the “Location and geological setting”-section and designed Figs. 1, 2, 5, 8. JS helped to draft the manuscript, participated in the field study and collected data and samples. SW led and coordinated the whole study and helped to design the draft.

Funding Open Access funding enabled and organized by Projekt DEAL. Not applicable.

Availability of data and materials All data are given in the supplement.

Declarations

Conflict of interest The authors declare that they have no competing interests.

Open Access This article is licensed under a Creative Commons Attribution 4.0 International License, which permits use, sharing, adaptation, distribution and reproduction in any medium or format, as long as you give appropriate credit to the original author(s) and the source, provide a link to the Creative Commons licence, and indicate if changes were made. The images or other third party material in this article are included in the article's Creative Commons licence, unless indicated otherwise in a credit line to the material. If material is not included in the article's Creative Commons licence and your intended use is not permitted by statutory regulation or exceeds the permitted use, you will need to obtain permission directly from the copyright holder. To view a copy of this licence, visit <http://creativecommons.org/licenses/by/4.0/>.

References

- Abraham de Vazquez EM., Garleff K, Liebricht H, Regairaz AC, Schäbitz F, Squeo, FA, Helmut S, Heinz V, Villagrán C (2000) Geomorphology and paleoecology of the arid diagonal in southern South America. *Zeitschrift für angewandte Geologie* 55–61
- Baldis B (1975) Acerca de la estructura profunda de la Precordillera Central. In: *Revista de Geología Mineralogía y Minería*, vol 23, pp 1–2. Buenos Aires
- Baldis B, Chebli G (1969) Estructura profunda del área central de la Precordillera sanjuanina. In: *Actas 4° Jornadas Geológicas Argentina*, vol 1, pp 47–66. Buenos Aires
- Beer JA, Allmendinger RW, Figueroa DE, Jordan TE (1990) Seismic stratigraphy of a neogene piggyback basin, Argentina (1). *AAPG Bull* 74:1183–1202
- Buggisch W, Keller M, Lehnert O (2003) Carbon isotope record of Late Cambrian to Early Ordovician carbonates of the Argentine Precordillera. *Palaeogeogr Palaeoclimatol Palaeoecol* 195(3–4):357–373
- C.R.A.S: Centro Regional de Aguas Subterráneas (1982) Investigación hidrogeológica en el valle de Iglesia. Province of San Juan. Publication N° P-245. Comprehensive preliminary report. C.R.A.S May of 1982
- Cahill T, Isacks BL (1992) Seismicity and shape of the subducted Nazca Plate. *J Geophys Res* 97:17503
- Cardó R, Díaz IN (1999) Hoja Geológica 3169-I Rodeo, Provincia de San Juan, Programa Nacional de Cartas de la República Argentina 1:250.000. Servicio Geológico Minero Argentino Instituto de Geología y Recursos Minerales, Buenos Aires
- Cloetingh SAPL, Van Balen RT, Ter Voorde M, Zoetemeijer BP, Den Bezemer T (1997) Mechanical aspects of sedimentary basin formation: development of integrated models for lithospheric and surface processes. *Geol Rundsch* 86(2):226–240
- Concha G, Broberg K, Grandier M, Cardozo A, Palm B, Vahter M (2010) High-level exposure to lithium, boron, cesium, and arsenic via drinking water in the Andes of Northern Argentina. *Environ Sci Technol* 44(17):6875–6880
- Contreras VH, Damiani O, Milana JP, Bracco A, Barrera OM (1990) Paleógeno y Neógeno de San Juan. En Bordonaro O (eds) *Relatorio Geología y Recursos Naturales de la Provincia de San Juan*, pp 154–185. 11° Congreso Geológico Argentino. San Juan
- DeMets C, Gordon RG, Argus DF, Stein S (1990) Current plate motions. *Geophys J* 101:425–478
- Dimitrov LI (2002) Mud volcanoes—the most important pathway for degassing deeply buried sediments. *Earth Sci Rev* 59(1–4):49–76
- Drever J (1996) Weathering processes. In: Saether O, de Caritat P (eds) *Geochemical processes, weathering and groundwater recharge in catchments*, Chapter 1. CRC Press, London
- Furque G (1979) Descripción geológica de la hoja 18c, Jachal (Prov. de San Juan). Dirección Nacional De Geología y Minería Boletín 125:1–79
- Gagliardo ML, Caselli AT, Limarino CO, Colombo F, Tripaldi A (2001) The tertiary units of the Rodeo-Iglesia Basin: validity and correlation of the formational units. *Revista De La Asociacion Geologica Argentina* 56(1):121–125
- Gibbs RJ (1970) Mechanisms controlling world water chemistry. *Science* 170(3926):1088–1090
- Gonzalez M, Clavel F, Christiansen R, Gianni GM, Klinger FL, Martinez P, Díaz M (2020) The Iglesia basin in the southern Central Andes: a record of backarc extension before wedge-top deposition in a foreland basin. *Tectonophysics* 228590
- Gregori SD, Christiansen R (2017) Seismic hazard analysis for central-western Argentina. *Geodesy Geodyn*. <https://doi.org/10.1016/j.geog.2017.07.006>
- Heredia N, Rodríguez Fernández L, Gallastegui G, Busquets P, Colombo F (2002) Geological setting Argentine Frontal Cordillera in the flat-slab segment (30°00′–31°30′). *J S Am Earth Sci* 15:79–99
- Jebreen H, Banning A, Wohnlich S, Niedermayr A, Ghanem M, Wisotzky F (2018) The influence of Karst Aquifer mineralogy and geochemistry on groundwater characteristics: West Bank Water, Palestine. <https://doi.org/10.3390/w10120000>
- Jordan TE, Allmendinger RW, Damanti JF, Drake RE (1993) Chronology of motion in a complete thrust belt: the Precordillera, 30–31 S, Andes Mountains. *J Geol* 101:135–156
- Keller M (1999) Argentine Precordillera: sedimentary and plate tectonic history of a Laurentian crustal fragment in South America. *Geol Soc Am Spec Publ* 341:140
- Keller M, Buggisch W, Lehnert O (1998) The stratigraphic record of the Argentine Precordillera and its plate-tectonic background. In: Pankhurst RJ, Rapela CW (eds) *The Proto-Andean Margin of the Gondwana*, vol 142. *Geol. Soc. London Spec. Publ.*, pp 35–56
- Kopf AJ (2002) Significance of mud volcanism. *Rev Geophys* 40:2-1-2–52
- Kopf AJ (2008) Making calderas from mud. *Nat Geosci* 1:500–501
- Llambías EJ, Sato AM (1990) El batolito de Colangüil (29°–31°S), Cordillera Frontal de Argentina: Estructura y marco tectónico. *Revista Geológica De Chile* 17(1):89–108
- Manga M, Brumm M, Rudolph ML (2009) Earthquake triggering of mud volcanoes. *Mar Pet Geol* 26:1785–1798
- Mazzani A, Etiope G (2017) Mud volcanism: an updated review. *Earth-Sci Rev* 168:81–112
- Meybeck M (1987) Global chemical weathering of surficial rocks estimated from river dissolved loads. *Am J Sci* 287:401–428
- Moek IS (2014) Catalog of geothermal play types based on geologic controls. *Renew Sustain Energy Rev* 37:867–882
- Mpodozis C, Ramos V (1989) The Andes of Chile and Argentina. In: *Geology of the Andes and its relation to hydrocarbon and mineral resources*; Erickson GE, Cañas MT and Reinemund, JA (eds) *Circum-pacific council for energy and mineral resources*, Houston, Texas Earth Science Series, vol 11, pp 59–90
- O'Reilly J, Watts MJ, Shaw RA, Marcilla AL, Ward NI (2010) Arsenic contamination of natural waters in San Juan and La Pampa, Argentina. *Environ Geochem Health* 32:491–515
- Perucca LP, Bastias H (2005) El Terremoto Argentino de 1894: Fenómenos de Licuefacción asociados a Sismos. *INSUGEO Serie Correlación Geológica* 19:55–70
- Perucca LP, Martos LM (2012) Geomorphology, tectonism and quaternary landscape evolution of the central Andes of San Juan (30°SE 69°W), Argentina. *Quatern Int* 253:80–90
- Perucca LP, Moreiras S (2006) Liquefaction phenomena associated with historical earthquakes in San Juan and Mendoza Provinces, Argentina. *Quat Int* 158(1):96–109
- Pesce AH, Miranda F (2003) Catálogo de Manifestaciones Termales de la República Argentina. Volume I, Northwest region. Provinces of

- Jujuy, Salta, Catamarca, Tucumán, Santiago del Estero, La Rioja and San Juan
- Polanski J (1970) Carbónico y Pérmico de la Argentina. Editorial of the Universidad de Buenos Aires, p 216
- Ramos VA, Cegarra ML, Cristallini E (1996) Cenozoic tectonics of the High Andes of west/central Argentina (30°–36° S latitude). *Tectonophysics* 259:185–200
- Ramos VA, Cristallini EO, Pérez DJ (2002) The Pampean flat-slab of the Central Andes. *J S Am Earth Sci* 15:59–78
- Ré GH, Jordan TE, Kelley S (2003) Cronología y paleogeografía del terciario de la cuenca intermontana de iglesia septentrional, Andes de San Juan, Argentina. *Revista De La Asociación Geológica Argentina* 58:31–48
- Rolleri E, Baldis B (1967) Paleogeography and distribution of carboniferous deposits in the Argentine Precordillera. En Coloquio de la I.U.G.S.: La Estratigrafía del Gondwana, Ciencias de la Tierra, vol 2, pp 1005–1024, UNESCO, 1969
- Rudolph ML, Manga M (2012) Frequency dependence of mud volcano response to earthquakes. *Geophys Res Lett.* <https://doi.org/10.1029/2012GL052383>
- Ruskin BG, Jordan TE (2007) Climate change across continental sequence boundaries: paleopedology and lithofacies of Iglesia basin, northwestern Argentina. *J Sediment Res* 77:661–679
- Smedley PL, Kinniburgh DG (2002) A review of the source, behaviour and distribution of arsenic in natural waters. *Appl Geochem* 17:517–568
- Srinivasamoorthy K, Vasanthavigar M, Chidambaram S, Anandhan P, Sarma VS (2011) Characterization of groundwater chemistry in an eastern coastal area of Cuddalore district, Tamil Nadu. *J Geol Soc India* 78(6):549–558
- Tinivella U, Giustiniani M (2012) An overview of mud volcanoes associated to gas hydrate system. In *Tech Open, Updates in volcanology—new advances in understanding volcanic systems*, edited by Karoly Nemeth, ISBN: 978-953-51-0915-0
- Wetten C (1975a) Geología del valle de Iglesia, su relación con los yacimientos de diatomita de Lomas del Campanario e importancia económica. Trabajo Final de Licenciatura, Facultad de Ciencias Exactas, Físicas y Naturales, Universidad Nacional de San Juan, p 70 (inédito)
- Wetten C (1975b) Estudio geológico-económico de un yacimiento de diatomitas y análisis de Mercado. In: 2º Congreso Iberoamericano de Geología Económica, Buenos Aires, pp 513–529
- World Health Organization (2011) Guidelines for drinking-water quality, 4th edn. WHO Library Cataloguing-in-Publication Data
- Yrigoyen MR (1972) Cordillera Principal. En Leanza AF (ed) *Geología Regional Argentina*, Academia Nacional de Ciencias. Córdoba, pp 345–364
- Zambrano J, Torres E (1996) Hidrogeología de la Provincia San Juan. *Catálogo de Recursos Humanos e Información Relacionada con la Temática Ambiental.* <https://www.mendoza-conicet.gob.ar/ladyot/catalogo/cdandes/cap12.htm#inhalt>. 14 Mar 2020